energies

MDPI

Article

Electro-Hydraulic Variable-Speed Drive Network Technology—First Experimental Validation

Lasse Schmidt * and Mikkel van Binsbergen-Galán

AAU Energy, Aalborg University, Pontoppidanstraede 111, 9220 Aalborg, Denmark; mbg@energy.aau.dk
* Correspondence: lsc@energy.aau.dk; Tel.: +45-2232-2622

Abstract: The improvement of the energy efficiency of hydraulic systems remains an essential challenge for industry, and the demand for more sustainable solutions is increasing. A main focus in this endeavor is the ability to eliminate or strongly reduce the use of throttle control valves which have been the preferred control element in industrial hydraulic systems for decades. Components have been subject to continuous evolution, and current industrial grade hydraulic pumps and motors are both efficient and reliable. Even though few percentages of energy efficiency can still be achieved, the main achievements in terms of efficiency are associated with novel system designs rather than further development of components. An area subject to increasing attention is the field of variable-speed displacement control, allowing to avoid the main control valve throttle losses. Systems using this technology are, however, mainly developed as standalone drive systems, necessitating maximum force, speed, and power installed in each axis, with limited hydraulic power distribution capability compared to valve-controlled systems. An emerging field addressing this challenge is that of so-called electro-hydraulic variable-speed drive networks, which allow to completely eliminate the use of control valves and enable power sharing both electrically and hydraulically, potentially reducing the necessary installed power in many cases. The idea of such a technology was first proposed in 2022, and so far developments reported in the literature have mainly been of a theoretical nature. This article presents the first ever experimental results for a dual-cylinder electro-hydraulic variable-speed drive network prototype. The prototype was developed for an industrial application, but has initially been implemented in a laboratory testbench. Extensive data acquisition has been conducted while subject to the associated industrial motion cycle, under different load conditions. The data obtained are further used in combination with models to predict the total efficiency of the drive network prototype under higher loads than what could be achieved in the laboratory, suggesting a total efficiency from the electric supply to the cylinder pistons of 68%. Re-configuring the prototype to a known standalone drive system structure implies comparable efficiencies. Finally, the drive network is theoretically compared to a valve drive solution, generally suggesting that the prototype drive network can provide efficiency improvements of at least 40% in comparison.

Keywords: electro-hydraulic variable-speed drive networks; electro-hydraulic cylinder drives; energy efficiency; power sharing; hydraulic actuation; linear actuation

check for updates

Citation: Schmidt, L.; van Binsbergen-Galán, M. Electro-Hydraulic Variable-Speed Drive Network Technology—First Experimental Validation. *Energies* **2024**, *17*, 3192. https://doi.org/10.3390/en17133192

Academic Editor: Andrey A. Kurkin

Received: 11 May 2024
Revised: 12 June 2024
Accepted: 25 June 2024
Published: 28 June 2024

Copyright: © 2024 by the authors. Licensee MDPI, Basel, Switzerland. This article is an open access article distributed under the terms and conditions of the Creative Commons Attribution (CC BY) license (https://creativecommons.org/licenses/by/4.0/).

1. Introduction

Throttle control valves have been the preferred control elements in hydraulic systems for decades. However, facing the current climate crisis, the high losses associated with this control approach pose a serious challenge for the industry. Hence, efforts to develop more efficient hydraulic drive technologies are increasing. Here, digital hydraulic displacement and flow control as well as variable-speed electro-hydraulic displacement control are the main focus areas.

The success of digital hydraulic technology is dependent on the successful development of new components, especially sufficiently fast switching valves [1–3], and has been reported to be successfully applied in different applications [4–11]. Despite these

efforts which have been ongoing for nearly four decades, this technology has yet to make a broad breakthrough in industry. The reason may be associated with the inherent flow switching that may challenge system controllability and performance, as well as the use of non-mass-produced components that may cause the technology to be cost-intensive compared to alternative approaches. A more recent contribution in this field is the so-called digital hydraulic oscillation transformer [12] using fewer and more simple components, potentially allowing to overcome these challenges. However, this technology is still at an early stage in its development.

Where digital hydraulic technology relies on switching valves with special features not necessarily available in industry, variable-speed electro-hydraulic displacement control technology mainly relies on well-known components in terms of electric motors, inverters, and hydraulic pumps and/or motors, realizing so-called variable-speed displacement units (VsDs). The main challenges in this area are how to design hydraulic systems without the use of throttle valves while achieving the desired functionalities for specific applications. The technology has mainly evolved as single-cylinder drives i.e., standalone drives, and several solutions have been reported in the literature, e.g., with single electric motor/single displacement units [13–15] including tandem displacement unit solutions [16,17], as well as solutions comprising two electric motors and two displacement units [18,19]. Also, drive solutions incorporating regenerative capabilities have been reported [20–22]. While these solutions are developed as single-axis drives, attention to multi-axis solutions is more limited in the literature. This field is, however, under development, including, e.g., VsDs combined with directional valves [23–26]. Also, the field of electro-hydraulic variable-speed drive networks is emerging after its first introduction in 2022 [27]. Since then, developments have focused on their control, component downsizing, design foundation in terms of load cycles, and application in construction machinery [28–31]. These drive networks are constructed from a number of VsDs connected to cylinder chambers in a *meaningful* way and potentially with the use of chamber short-circuits, effectively reducing the number of control volumes. These features enable electro-hydraulic power sharing that may lead to a reduced number of VsDs compared to standalone-type solutions, as well as potential downsizing of the associated power installations, dependent on the load requirements of the machine. So far, findings in this area have been of a theoretical nature.

This article presents the first experimental validation of an electro-hydraulic variable-speed drive network technology ever conducted. The experimental results are obtained from the first electro-hydraulic variable-speed drive network prototype ever realized, produced for actuation of a so-called industrial *moving floor* application comprising two cylinders. The prototype has been implemented in a laboratory testbench made for the specific purpose of validating the basic functionalities of the drive network prototype, with a main emphasis on motion and system sum-pressure control, as well as power consumption and efficiency. The cylinders of the industrial application are rather large and able to produce rather high forces, though the possibility to apply loads under laboratory conditions has been limited. For this reason, the prototype laboratory validation only encompass part load operation while the motion pattern and cycle frequency of the industrial application are maintained. Hence, besides validating the prototype experimentally, the efficiency properties under higher loads are predicted using data-aided model-based analyses and, furthermore, are compared to a standalone electro-hydraulic drive solution. Finally, the prototype is theoretically compared to a conventional valve-controlled drive solution.

2. Dual-Cylinder Electro-Hydraulic Variable-Speed Drive Network Testbench

The dual-cylinder electro-hydraulic variable-speed drive network (EDN) testbench is shown in Figure 1, where (Figure 1A) depicts the functional schematics of the testbench and (Figure 1B) shows a picture of the physical testbench. The testbench comprises two cylinders with a short circuit of the piston-side cylinder chambers, ideally resulting in three control volumes which may be controlled by three (pairs of) VsDs. As mentioned above, the EDN has been developed for a moving floor application, allowing this to be

demonstrated in an industrial environment. The moving floor application is subject to large cylinders and motion cycle frequencies up to 16 cycles/min, resulting in high flow requirements for the drive system. Hence, to realize the functionality with standard electric drives, each VsD function is realized as a pair of identical VsDs, i.e., there are six VsDs with these operated as three. The VsDs connected to the hydraulic tank are denoted *supply units* (SU1 and SU2), while the VsDs that are connected between the cylinder chambers are denoted *drive units* (DU1.1, DU1.2, DU2.1 and DU2.2), as depicted in Figure 1. Hence, when operated in pairs, this means that drive units DU1.1, DU1.2 are subject to the same speed command and similarly with DU2.1, DU2.2 and SU1, SU2.

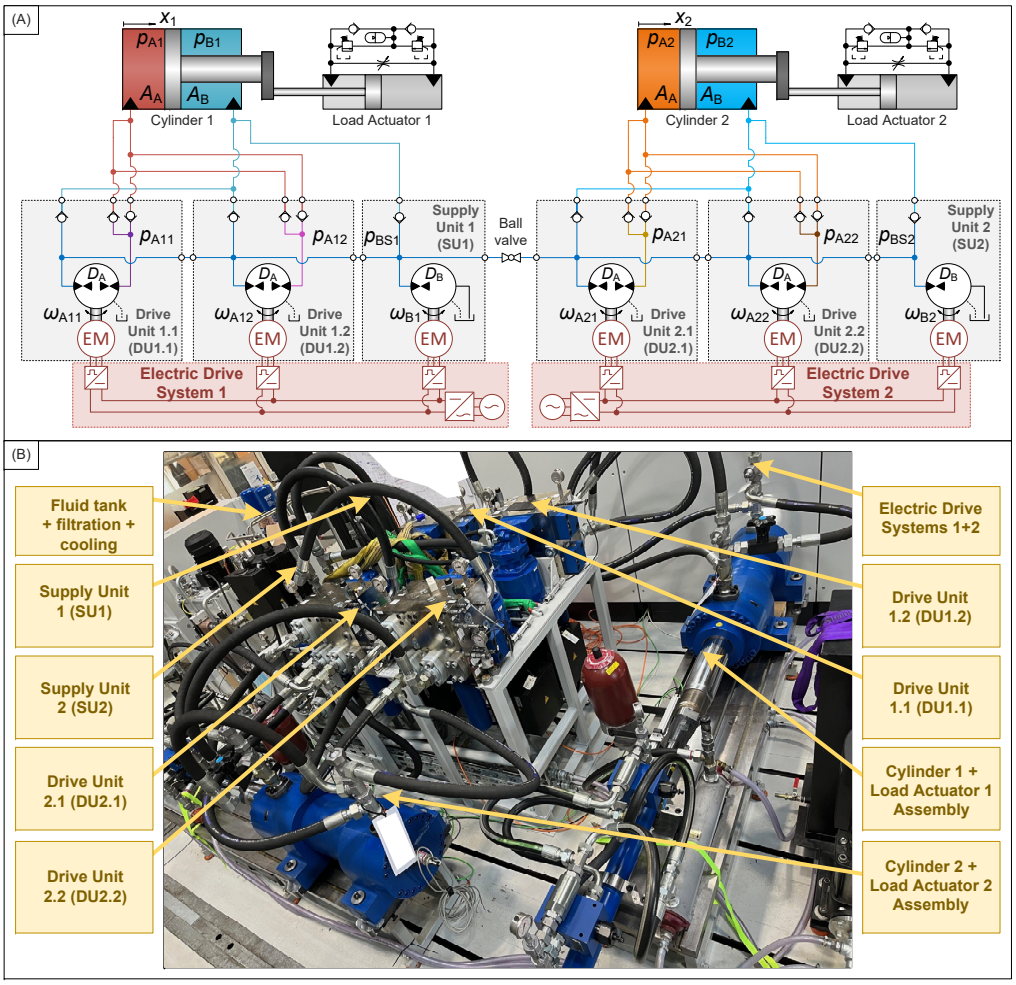


Figure 1. Dual-cylinder electro-hydraulic variable-speed drive network prototype. (**A**) Functional schematics. (**B**) Physical laboratory testbench illustration.

The industrial moving floor application is subject to lengthy fluid lines between the EDN and the cylinders. Hence, to ensure a reasonable level of fluid filtration and cooling at the fluid tank level, a fluid exchange mechanism was realized comprising parallel lines between the EDN and the cylinders, with check valve functions ensuring separate flow paths to and from the cylinders and the EDN. This functionality increases the transmission losses compared to standard fluid lines, but prevents excessive heating of the fluid.

For laboratory tests and functional validation, the load forces are realized by *passive* load actuators with limited force capabilities, established via pressure relief valves. This is not an ideal load mechanism for two main reasons: (1) The inertia masses are rather low, and with the back-to-back mechanically coupled cylinder/load actuators, the eigenfrequencies of these assemblies become high relative to the industrial moving floor application. (2) The cylinders of the load actuators have substantially smaller diameters compared to the *main*

cylinders (see Table 1); hence, only limited load forces can be applied to the main cylinders. However, the test setup does allow to validate the basic controllability of the EDN, the main transmission losses under part load, etc., rendering the test bench feasible for experimental validation of the basic technology. Finally, the main components used in the testbench are listed in Table 1.

Table 1. Main components of dual-cylinder electro-hydraulic variable-speed drive network testbench drive. [a] Bosch Rexroth AG, Lohr am Main, Germany [b] Balluff ApS, Aalborg, Denmark.

Configuration	Description	Pcs.
[a] A2FMM125/70	Hydraulic bent axis motor used in Drive Units	4
[a] PGH5-3X/100	External gear pump used in Supply Units	2
[a] LC40A10E7X/	Logic cartridge valves (check valve functions)	2
[a] HM 20-2X/	Pressure sensor (various ranges)	8
[b] BTL7-V50E-M1000-P-C003	Position sensor (etherCAT)	2
[a] Cylinder: 220/140-400 [mm]	Cylinder 1 and 2	2
[a] Cylinder: 80/56-770 [mm]	Cylinder of load actuator 1 and 2	2
[a] MS2N13-E1BHL-CSEG0	Electric motor used in Drive and Supply Units	6
[a] ctrlX XVR2-W0072ARN	Electric power supply	2
[a] ctrlX XMS2-W0250ANN	Electric inverter drive used in Drive Units	4
[a] ctrlX XMS2-W0210ANN	Electric inverter drive used in Supply Units	2
[a] ctrlX Core	Control hardware for control software implementation	1

3. Experimental Results, Efficiencies, and Comparisons

For experimental validation of the main EDN functionality, the prototype is controlled using the control structure proposed in [29]. The prototype is operated with a motion pattern identical to that of the moving floor application, with the highest motion cycle frequency, i.e., 16 cycles/min. Under these motion conditions, 12 different load cases have been realized using different pressure relief valve settings, as specified in Table 2, where it should be noted that the pressure relief valves have been adjusted manually and with the use of an analogue manometer for pressure monitoring.

Table 2. Pressure relief valve settings for the tests conducted.

Test #	Pressure Relief Valve Setting	Test #	Pressure Relief Valve Setting
1	All relief valves @ 0 [MPa], orifices open	7	All relief valves ≈ 10.0 [MPa]
2	All relief valves ≈ 1.0 [MPa]	8	All relief valves ≈ 12.0 [MPa]
3	All relief valves ≈ 1.5 [MPa]	9	All relief valves ≈ 14.0 [MPa]
4	All relief valves ≈ 4.0 [MPa]	10	All relief valves ≈ 16.0 [MPa]
5	All relief valves ≈ 6.0 [MPa]	11	All relief valves ≈ 18.0 [MPa]
6	All relief valves ≈ 8.0 [MPa]	12	All relief valves ≈ 20.0 [MPa]

For detailed inspection, the relevant states of the testbench are depicted in Figure 2 for Test # 12. From Figure 2D–F, it is evident that the piston positions track their references with reasonable precision considering its industrial application, and the instantaneous lower chamber pressure is maintained in the vicinity of its pressure setting of 2.0 [MPa]. Furthermore, it is notable that the piston pressure forces depicted in Figure 2B do not settle at a zero value even though the cylinders are horizontally mounted. The reason is that the control is subject to steady-state position errors, causing the controller to provide a small input to the electric drives, and consequently, the pistons literally always move under these motion cycles, at least with a very low velocity. Therefore, the load actuator pistons also move, and the associated pressures, hence forces, are maintained at levels corresponding to the pressure relief valve settings. When the cylinder pistons are controlled in the reverse direction, the pressure is relieved and the force reduced. However, the forces are not instantly increased in the reverse direction as the associated load actuator chambers need

to be compressed before the relief valve cracking pressures are reached. These properties comprise the main differences from the load in the industrial application.

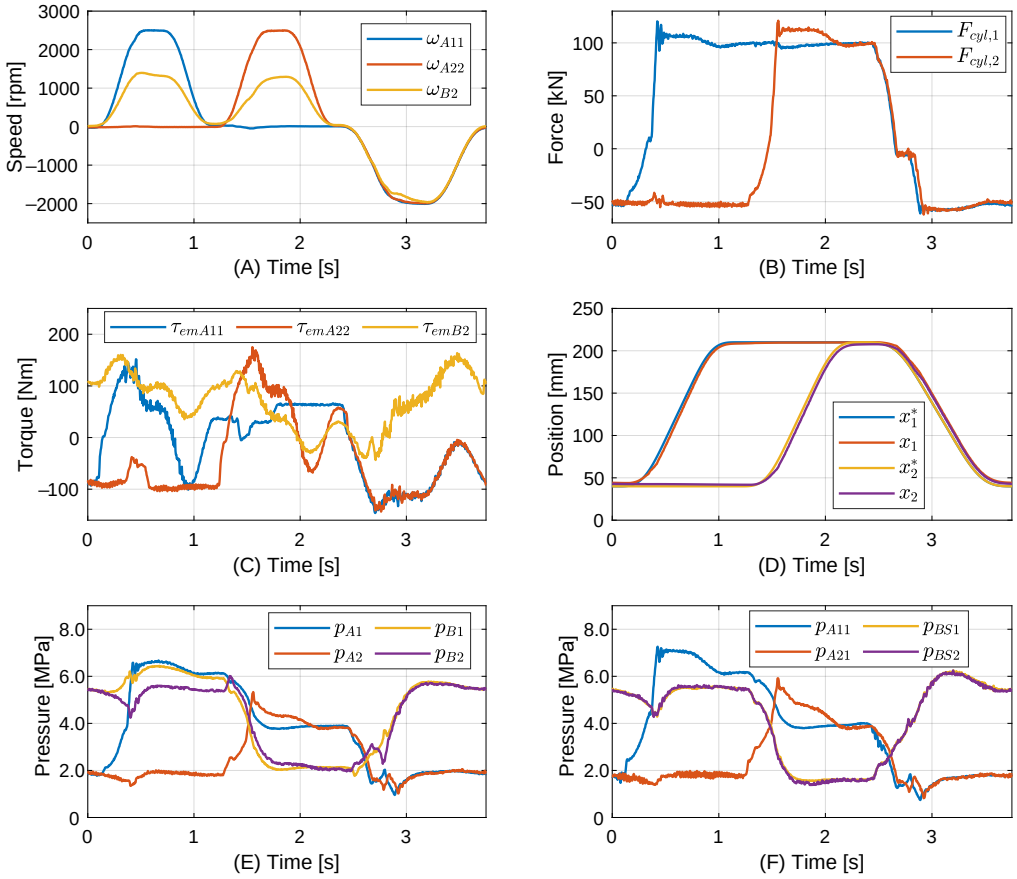


Figure 2. EDN states for Test # 12 operating at 16 motion cycles per minute. (**A**) Actual EM shaft speeds. (**B**) Hydraulic pressure forces of main cylinder pistons. (**C**) EM electro-magnetic torques. (**D**) Main cylinder piston positions and position commands (marked with superscript *). (**E**) Chamber pressures of main cylinders. (**F**) EDN side pressures.

Considering the electro-magnetic torques of the electric motors (EM's) in Figure 2C, these are subject to larger transients than the hydraulic pressure forces of the main cylinder pistons. The reason for this is the large acceleration torques required by the EMs compared to the necessary acceleration forces of the cylinder pistons. This is due to the relatively large inertia of the combined rotary group of each VsD compared to the inertia mass of the cylinder/load actuator assemblies. Finally, the EM shaft speeds depicted in Figure 2A appear well behaved with the different maximum positive and negative speeds owed to the different main cylinder piston velocity requirements for piston extension and retraction.

The power at different points in the system during a single motion cycle for all 12 tests, is shown in Figure 3 along with the associated piston forces. First, it is found from the piston forces in Figure 3A,B, that the load actuator forces behave similarly to the description above in all tests. From Figure 3C,D, depicting the total power associated with the main cylinder pistons and the displacement unit outlets, these are found to have similar behavior. However, considering the total DC-bus power depicted in Figure 3E, the power associated with acceleration/deceleration of the EMs is clearly seen. Part of the power associated with deceleration of the EM shaft is passed towards the electric supply, and the energy intermediately stored in the supply capacitance.

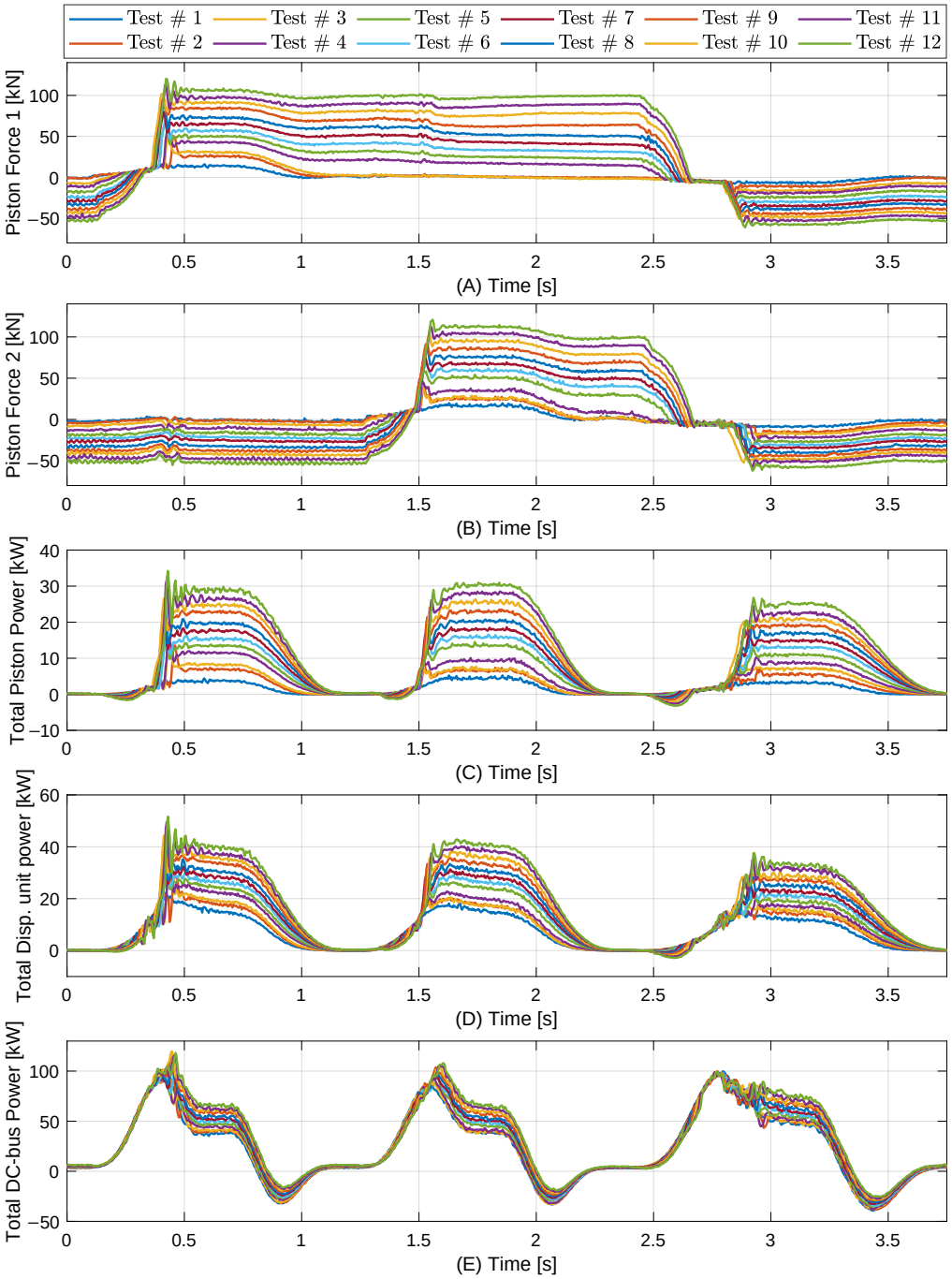


Figure 3. Force and power measures for all 12 EDN tests. (**A**) Hydraulic pressure forces of main cylinder 1. (**B**) Hydraulic pressure forces of main cylinder 2. (**C**) Total hydraulic output power of both cylinder 1 and cylinder 2. (**D**) Total displacement unit output power of all VsDs. (**E**) Total power of both electric supplies (DC-bus's).

Consider now specifically the hydraulic piston output power, the displacement unit output power and the DC-bus power of the electric supplies for Test # 12, depicted in Figure 4. Noting also the shaft speed example of Figure 2A, it is found that the DC-bus power associated with EM shaft acceleration is subject to a transient, approximately 65% higher than the subsequent period of nearly constant speeds. However, as also found from Figure 4, the average DC-bus power is only approximately a third of the DC-bus peak power. The relatively large EM acceleration power level sets high requirements to the DC-bus peak power capacity, a feature that generally must be considered in detail for electro-hydraulic variable-speed drives to ensure that the intended performance is achievable.

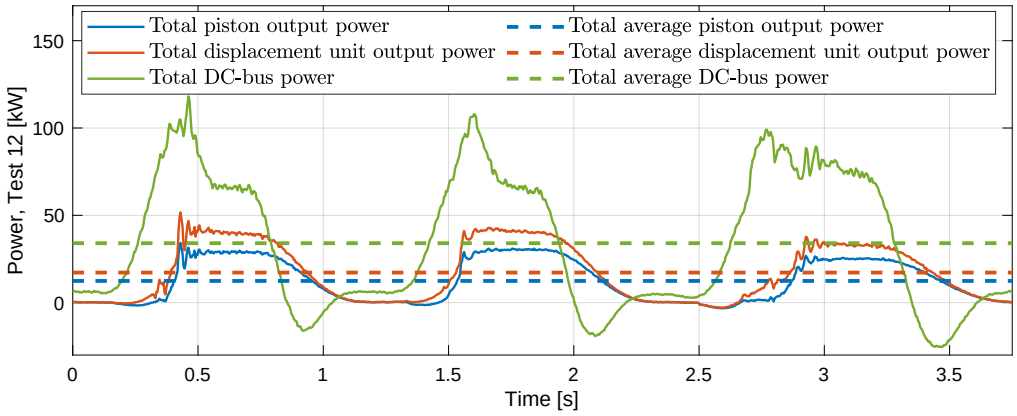


Figure 4. EDN power measures, including average levels, for Test # 12.

3.1. Comparison with Standalone Electro-Hydraulic Variable-Speed Drive System

Having considered the general performance features as well as the power characteristics of the EDN, it is relevant to consider its general properties and efficiencies when compared to standalone electro-hydraulic drive solutions. The standalone electro-hydraulic drive (SED) solution considered here is similar to the one presented in, e.g., [18], and is realized with the EDN testbench by closing the ball valve depicted in the schematics of Figure 1. This disables the short-circuit connection between the two cylinders, thereby removing the hydraulic coupling.

The main differences between the EDN and SED are associated with the supply unit functionality and whether the piston-side chambers are short-circuited as for the EDN or not as for the SED. Considering the DUs, these have to displace the same amount of fluid with respect to time and, hence, the associated flows for the EDN and SED closely resemble each other. However, for the EDN, SU1 and SU2 operate as a single unit connected to the common piston-side volume, whereas for the SED the SUs are operated separately. Hence, the EDN supply unit function is realizable with less but larger components, is potentially subject to less losses due to fewer transmission interfaces, and definitely entails less system integration effort.

The average efficiencies for the EDN and SED for the 12 test scenarios are calculated from the power measures and are depicted in Figure 5. From an efficiency point of view, the EDN and SED appear nearly identical. This is to be expected as the two drive system architectures are physically similar, contain the same components, and perform the same output work. Considering specifically the EDN, the measured maximum average efficiencies are obtained under the maximum loads applied, with increasing trend, suggesting higher efficiencies at higher loads. The measured maximum average efficiencies from mains to electric motor shafts, electric motor shafts to displacement machine outlets, and displacement machine outlets to cylinder pistons are obtained as 81%, 62%, and 72%, respectively, with a measured total maximum average efficiency from mains to cylinder pistons of 37%.

Discussion

The efficiency measures appear rather low, bearing in mind the absence of proportional control valves and, hence, conceptual losses. However, noting the pressure levels depicted in Figure 2, i.e., the test with the highest external load force, it may be clear that the drive systems and the actuators are only subject to minor loads. As an example, the bent axis hydraulic motors are designed for a nominal speed of 4000 [rpm] and a nominal pressure difference of 40.0 [MPa], while the maximum shaft speed and pressure difference achieved in the tests are approximately 2510 [rpm] and 4.6 [MPa], respectively. Hence, the bent axis hydraulic motors are indeed operated at part load, with the maximum speed and pressure difference being just 63% and 12% of their nominal ranges. For this reason the losses are relatively high compared to their outputs. Furthermore, the pressure losses in

the pipes/hoses and fluid exchange mechanisms are mainly associated with the flows and, hence, the motion cycles. Therefore, as the pressures are low, the associated losses are relatively high compared to the transmitted power. The expected efficiencies at higher loads are considered in the subsequent section.

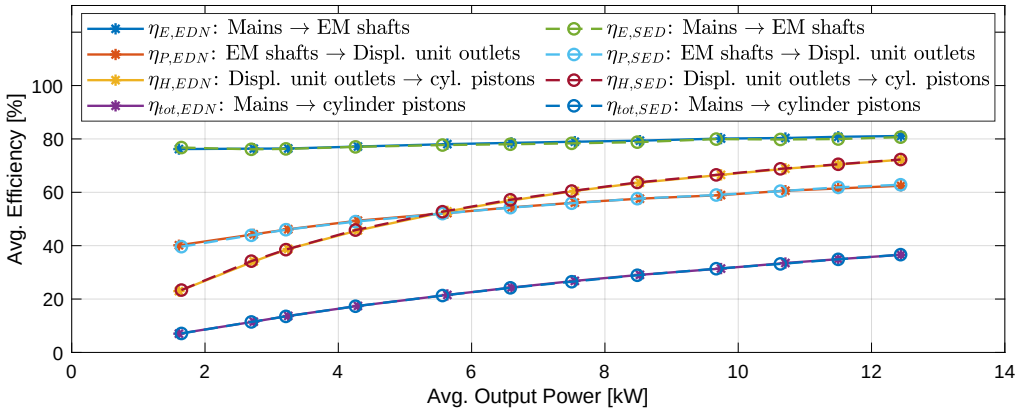


Figure 5. Measured average efficiencies at different points in the EDN and SED, at 16 cycles/min and all 12 load test cases.

3.2. Efficiency Prediction at Increased External Loads

In order to provide a prediction of the efficiency at higher load forces, models aided by experimental data are applied. Considering the losses of the pipe/hose/fluid exchange mechanisms, the modeling of these may be subject to substantial uncertainties, mainly due to the complexity of the logic cartridge valves used to realize the check functions. However, as the associated losses are mainly related to the flows and, hence, motion cycles, the measured losses are used while compensating for the effect of increased pressures. As reliable loss models for the used displacement units have not been available, the loss model of a Bosch Rexroth A4FM fixed displacement axial piston motor presented in [27] is used as a basis for all six displacement units of the EDN. Here, the source data for the measured losses originate from [32], and are dependent on shaft speeds and pressure differences across the displacement units. Hence, basically, it is assumed that the cross-port leakage, drain flows, and friction for all the displacement machines used develop similarly to the A4FM as a function of the shaft speed and pressure difference, and are subsequently scaled to fit the measured data on the EDN. Firstly, the leakage model was scaled according to the external leakage flows calculated from Equation (1) for all the tests, as this measure accounts for all drain flows and other external leakages at a systems level. Secondly, the friction model was scaled to fit the measured displacement unit output power at a systems level.

$$Q_{\Sigma\text{loss}} = D_\text{B}(\omega_{\text{B}1} + \omega_{\text{B}2}) - (A_\text{A} - A_\text{B})(\dot{x}_1 + \dot{x}_2) \tag{1}$$

Considering the electric system, no reliable loss model information has been available, and hence, this is left out of the analysis. However, the combined efficiency of these components is expected to increase to above 90% when properly loaded.

In order to evaluate the efficiency at higher loads, models that scale the measured hydraulic forces are applied. The increased forces are generated using the measured pressure data for Test # 12. As the procedure is identical for both cylinders, only the process for cylinder 1 is presented here. Let $p_{\text{A}1}$, $p_{\text{B}1}$ be the measured pressures associated with the measured pressure force $F_{\text{cyl}1} = A_\text{A} p_{\text{A}1} - A_\text{B} p_{\text{B}1}$, and let a scaled force be denoted

$\hat{F}_{\text{cyl1}} = k_s F_{\text{cyl1}}$, where k_s is a scaling factor. Then, the chamber pressures $\hat{p}_{\text{A1}}$, $\hat{p}_{\text{B1}}$ associated with the scaled force $\hat{F}_{\text{cyl1}}$, may be calculated by Equations (2) and (3).

$$\hat{p}_{\text{A1}} = \begin{cases} \dfrac{A_{\text{B}} p_{\text{B1}} + \hat{F}_{\text{cyl1}}}{A_{\text{A}}} & \text{for} \quad \hat{F}_{\text{cyl1}} \geq (A_{\text{A}} - A_{\text{B}}) \min(p_{\text{A1}}, p_{\text{B1}}) \\ \min(p_{\text{A1}}, p_{\text{B1}}) & \text{for} \quad \hat{F}_{\text{cyl1}} < (A_{\text{A}} - A_{\text{B}}) \min(p_{\text{A1}}, p_{\text{B1}}) \end{cases} \tag{2}$$

$$\hat{p}_{\text{B1}} = \begin{cases} \min(p_{\text{A1}}, p_{\text{B1}}) & \text{for} \quad \hat{F}_{\text{cyl1}} \geq (A_{\text{A}} - A_{\text{B}}) \min(p_{\text{A1}}, p_{\text{B1}}) \\ \dfrac{A_{\text{A}} p_{\text{A1}} - \hat{F}_{\text{cyl1}}}{A_{\text{B}}} & \text{for} \quad \hat{F}_{\text{cyl1}} < (A_{\text{A}} - A_{\text{B}}) \min(p_{\text{A1}}, p_{\text{B1}}) \end{cases} \tag{3}$$

Hence, the scaled force $\hat{F}_{\text{cyl1}}$ has the same *shape* as the measured force used, and the instantaneous lower pressure is identical to the corresponding measured pressure.

The predicted efficiencies are shown in Figure 6, demonstrating that the predicted and measured efficiencies closely resemble each other in the lower output power range. The main discrepancies between the measured and simulated efficiencies are related to the predicted displacement unit efficiencies, which slightly deviate at the lower output power levels. However, the main interest is the predicted efficiency from the EM shaft to the cylinder pistons depicted in Figure 6, suggesting a maximum efficiency for the considered motion cycle of approximately 77% from the EM shafts to the cylinder pistons at an average output power of 110 [kW]. The industrial moving floor application is, for the considered motion cycle, expected to have an average output power of 80 [kW], and, hence, a predicted efficiency from the EM shafts to the cylinder pistons of approximately 76%. Assuming a total average electric system efficiency of 90% under this load, the total average system efficiency from the electric supplies to the cylinder pistons is expected to be approximately 68%.

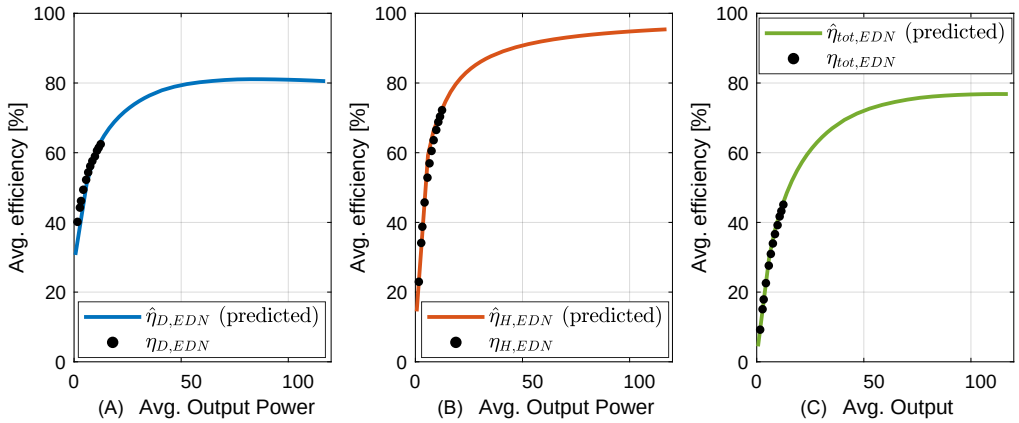


Figure 6. Predicted efficiencies for specified motion cycles and increased loads, and comparison with tests. (**A**) Total efficiency of all displacement units. (**B**) Total efficiency of all pipes/hoses/fluid exchange mechanisms. (**C**) Total efficiency from EM shafts to the main cylinder pistons.

3.3. Comparison with Valve Drive System Solution

Having compared the EDN to the SED, it is relevant also to compare the EDN to a conventional valve drive system solution. In the following, a drive system controlled by 4/3 proportional control valves fed by a variable-speed pump is denoted a *valve drive system* (VDS), with such a system depicted in Figure 7.

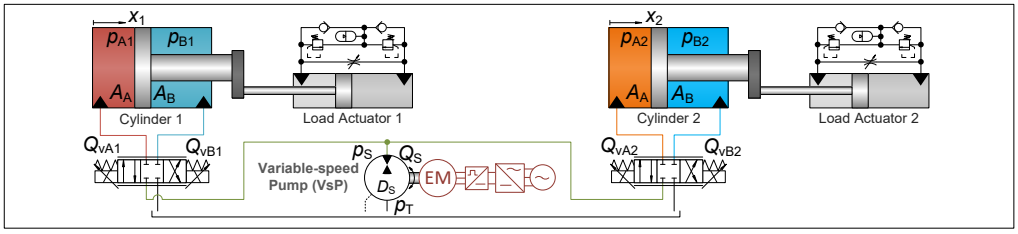


Figure 7. Schematics of proportional valve drive system fed by variable-speed pump (VDS).

To evaluate the power needed to provide the same work as the EDN, consider now the port flows for the valve associated with cylinder 1 given by Equations (4) and (5) for positive and negative piston motion, respectively. Here, x_{v1} is the associated spool position, k_v the valve flow gain, and σ the ratio of the valve port flow gains.

$$Q_{vA1} = k_v x_{v1}\sqrt{p_S - p_{A1}}\ ,\ \ Q_{vB1} = \sigma k_v x_{v1}\sqrt{p_{B1} - p_T} \quad \text{for} \quad \dot{x}_1 > 0 \tag{4}$$

$$Q_{vA1} = k_v x_{v1}\sqrt{p_{A1} - p_T}\ ,\ \ Q_{vB1} = \sigma k_v x_{v1}\sqrt{p_S - p_{B1}} \quad \text{for} \quad \dot{x}_1 < 0 \tag{5}$$

Under steady-state conditions and leakages absent at positive piston motion ($\dot{x}_1 > 0$), the flows Q_{vA1}, Q_{vB1} are related according to Equation (6), where $A_B = \alpha A_B$.

$$\begin{aligned} \alpha Q_{vA1} = Q_{vB1} \ &\Rightarrow\ \alpha k_v x_{v1}\sqrt{p_S - p_{A1}} = \sigma k_v x_{v1}\sqrt{p_{B1} - p_T} \\ &\Rightarrow\ \alpha^2(p_S - p_{A1}) = \sigma^2(p_{B1} - p_T) \end{aligned} \tag{6}$$

Indeed, for $\dot{x}_1 > 0$, the supply pressure must satisfy $p_S > p_{A1}$. This condition may be expressed as $p_S = p_\Delta + p_{A1}$, where p_Δ is some pressure margin necessary for the valve to realize the required flow. Using this, and the fact that $F_{cyl1} = A_A p_{A1} - A_B p_{B1}$, then from Equation (6), the supply pressure is obtained as Equation (7). Similarly, for $\dot{x}_1 < 0$, the supply pressure is given by Equation (8).

$$p_S|_{\dot{x}_1>0} = p_S = \frac{\alpha^3 + \sigma^2}{\sigma^2}p_\Delta + \alpha p_T + \frac{F_{cyl1}}{A_A} \quad \text{for} \quad \dot{x}_1 > 0 \tag{7}$$

$$p_S|_{\dot{x}_1<0} = p_S = \frac{\alpha^3 + \sigma^2}{\alpha^3}p_\Delta + \frac{p_T}{\alpha} + \frac{F_{cyl1}}{\alpha A_A} \quad \text{for} \quad \dot{x}_1 < 0 \tag{8}$$

Using a similar approach for cylinder 2 and its associated valve, the supply pressures appear as Equations (9) and (10).

$$p_S|_{\dot{x}_2>0} = p_S = \frac{\alpha^3 + \sigma^2}{\sigma^2}p_\Delta + \alpha p_T + \frac{F_{cyl2}}{A_A} \quad \text{for} \quad \dot{x}_2 > 0 \tag{9}$$

$$p_S|_{\dot{x}_2<0} = p_S = \frac{\alpha^3 + \sigma^2}{\alpha^3}p_\Delta + \frac{p_T}{\alpha} + \frac{F_{cyl2}}{\alpha A_A} \quad \text{for} \quad \dot{x}_2 < 0 \tag{10}$$

Hence, for a load sensing control function emulating that of conventional hydraulic power units, the necessary supply pressure may be estimated as Equation (11).

$$\hat{p}_S = \max(p_S|_{\dot{x}_1>0}, p_S|_{\dot{x}_1<0}, p_S|_{\dot{x}_2>0}, p_S|_{\dot{x}_2<0}) \tag{11}$$

The pump flow is estimated as Equation (12) and, hence, the pump outlet power is estimated as Equation (13).

$$\hat{Q}_S = \hat{Q}_{S1} + \hat{Q}_{S2} \tag{12}$$

$$\hat{Q}_{S1} = \begin{cases} A_A\dot{x}_1 & \text{for} \quad \dot{x}_1 \geq 0 \\ -A_B\dot{x}_1 & \text{for} \quad \dot{x}_1 < 0 \end{cases}\ ,\ \ \hat{Q}_{S2} = \begin{cases} A_A\dot{x}_2 & \text{for} \quad \dot{x}_2 \geq 0 \\ -A_B\dot{x}_2 & \text{for} \quad \dot{x}_2 < 0 \end{cases}$$

$$\hat{P}_S = \hat{p}_S\hat{Q}_S \tag{13}$$

Using the above, as well as the displacement unit loss model used in the previous section, $p_\Delta = 1.0$ [MPa], and assuming an efficiency of the electric system of 80% similar to the EDN measurements in Figure 5, the estimated efficiencies for the VDS compared to the EDN are depicted in Figure 8 for all 12 test cases. Here, both the case of using symmetric valves ($\sigma = 1$) and using matched valves ($\sigma = \alpha$) are presented.

Evidently, the efficiencies of the VDSs are lower than those of the EDN, which is mainly due to the fact that p_S is dictated by the highest chamber pressure plus p_Δ and the resulting throttle losses. In fact for, e.g., Test # 12, the total EDN efficiency is 22% and 66% higher than the efficiencies of the matched and symmetric VDSs, respectively.

Predicting the expected efficiencies similarly to the previous section, the results appear as depicted in Figure 9. It is found that the total VDS efficiencies never exceed 55% in any case for this system with the specified motion cycle, even when hose losses are neglected as considered here. Furthermore, it is notable that the EDN improves the system efficiency by ≈40% and ≈47% compared to the VDSs with matched and symmetric valves, respectively.

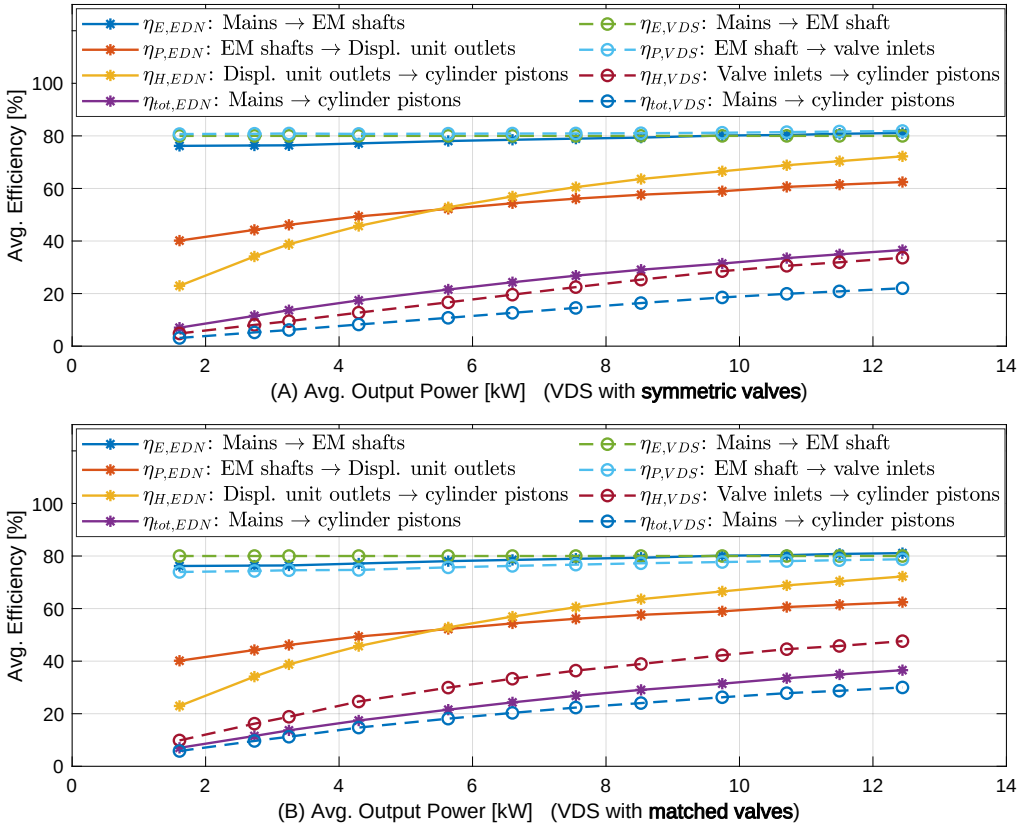


Figure 8. Measured average EDN efficiency measures, and VDS efficiency measures estimated from measured cylinder pressures and flows. (**A**) The EDN and VDS with symmetric valve spools. (**B**) The EDN and VDS with valve spools matched to the cylinder area ratios.

Discussion

The presented results are associated with the use of 4/3 valves in general and not any specific valves. This emphasizes the crucial importance of not only using variable-speed pumps in the endeavors to improve hydraulic system efficiencies, but to develop system architectures that do not rely on control valves in order to realize efficient hydraulic systems.

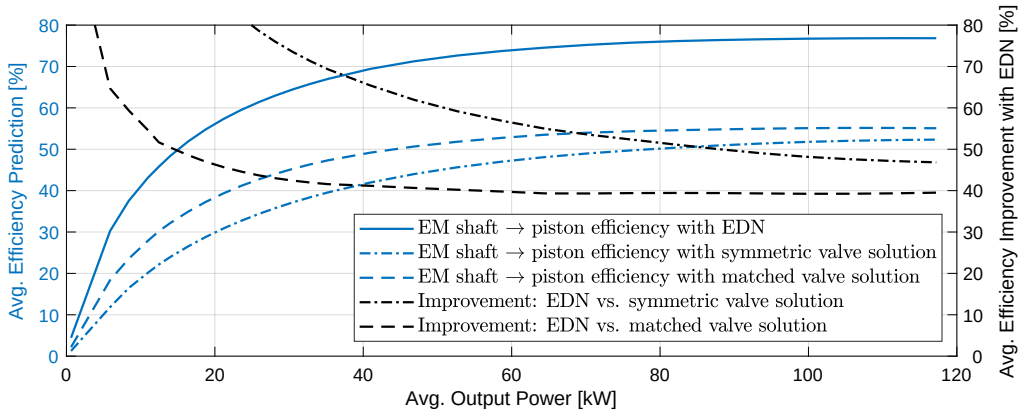


Figure 9. Predicted EM shaft-to-piston efficiencies with EDN and VDS solutions with symmetric and matched valves, and improvements with EDN compared to VDSs.

4. Conclusions

The first experimental results for electro-hydraulic variable-speed drive network technology are presented. This technology field has only recently been introduced, and developments presented in the literature have so far been of a theoretical nature, focusing on its key properties in terms of system control, downsizing capabilities, system design foundations, as well as application to a crane and a construction machine. In this article the first electro-hydraulic variable-speed drive network prototype ever built is presented. The prototype has been developed for a so-called moving floor application allowing demonstration in an industrial environment, and comprises two identical cylinders to be controlled. The electro-hydraulic variable-speed drive network prototype is realized with short-circuit of the rod-side cylinder chambers, and comprises three electric motor/displacement unit functions. However, due to large cylinder diameters and high motion cycle frequency requirements, the resulting flows are rather large, and due to the available component sizes, the prototype is realized with paired electric motors/displacement units in order to meet the flow requirements. Furthermore, as a consequence of the large cylinder diameters, only part loads are realizable by the load actuators under laboratory conditions. Experimental data have been acquired while conducting motion cycles associated with the industrial application, under twelve different load cases, and the results are presented, demonstrating feasible performance in terms of motion and pressure control. Also, the electro-hydraulic variable-speed drive network shows a total maximum efficiency of 37%, however, under the part loads realizable under laboratory conditions. Also, the experimental results from the electro-hydraulic variable-speed drive network prototype have been compared to those of a standalone electro-hydraulic drive system configuration, also showing a total maximum efficiency of 37%. Furthermore, as only part load tests have been realizable, data-aided models have been used to predict the total efficiency under higher loads. The results predict a total average efficiency from the electric supply to the cylinder pistons of 68%. Finally, the electro-hydraulic variable-speed drive network prototype is compared to a conventional valve drive solution, implying that a maximum efficiency under the considered load cycles of 55% is achievable with a valve solution. To this end, the electro-hydraulic variable-speed drive network prototype is found to provide efficiency improvements of at least 40% in comparison to a valve solution.

Author Contributions: Conceptualization, L.S.; methodology, L.S. and M.v.B.-G.; formal analysis, L.S. and M.v.B.-G.; investigation, L.S. and M.v.B.-G.; writing—original draft preparation, L.S.; writing—review and editing, L.S. and M.v.B.-G.; visualization, L.S.; project administration, L.S.; funding acquisition, L.S. All authors have read and agreed to the published version of the manuscript.

Funding: This research was funded by the Danish Energy Agency, the Energy Technology Development and Demonstration Programme, project: *Efficient Cement Handling Systems Based on Electro-Hydraulic Power Regeneration Networks* (eCHASPOR), project number 64020-2046.

Data Availability Statement: The data presented in this work are not available due to commercial considerations.

Conflicts of Interest: The authors declare no conflicts of interest.

Abbreviations

The following abbreviations are used in this manuscript:

EDN	Electro-hydraulic variable-speed drive network
EM	Electric motor
SED	Standalone electro-hydraulic variable-speed drive system
VDS	Valve drive system fed by electro-hydraulic variable-speed pump
VsD	Variable-speed displacement unit

Nomenclature

The following nomenclature are used in this manuscript:

A_{A}	Piston-side area of cylinder 1 and 2
A_{B}	Rod-side area of cylinder 1 and 2
D_{A}	Displacement of DU1.1, DU2.1, DU2.1 and DU2.2
D_{B}	Displacement of SU1 and SU2
F_{cyl1}	Hydraulic force estimate for cylinder piston 1
F_{cyl2}	Hydraulic force estimate for cylinder piston 2
k_{s}	Force scaling factor
k_{v}	4/3 valve flow gain
p_{A1}	Piston-side pressure of cylinder 1
p_{A2}	Piston-side pressure of cylinder 2
p_{A11}	Port pressure of displacement unit in DU1.1
p_{A12}	Port pressure of displacement unit in DU1.2
p_{A21}	Port pressure of displacement unit in DU2.1
p_{A22}	Port pressure of displacement unit in DU2.2
p_{B1}	Rod-side pressure of cylinder 1
p_{B2}	Rod-side pressure of cylinder 2
p_{BS1}	Port pressure of displacement unit in SU1
p_{BS2}	Port pressure of displacement unit in SU2
p_{S}	Supply pressure to 4/3 valves
p_{T}	Reservoir/tank pressure
p_{Δ}	Load sensing pressure margin
Q_{vA1}	Valve flow related to the piston side of cylinder 1
Q_{vB1}	Valve flow related to the rod side of cylinder 1
$Q_{\Sigma\mathrm{loss}}$	Total flow loss of EDN
$\dot{x}_1$	Velocity of cylinder piston 1
$\dot{x}_2$	Velocity of cylinder piston 2
x_{v1}	Spool position of 4/3 valve
α	Cylinder area ratio
σ	Ratio of 4/3 valve port flow gains
ω_{A11}	Shaft speed of displacement unit in DU1.1
ω_{A12}	Shaft speed of displacement unit in DU1.2
ω_{A21}	Shaft speed of displacement unit in DU2.1
ω_{A22}	Shaft speed of displacement unit in DU2.2
ω_{B1}	Shaft speed of displacement unit in SU1
ω_{B2}	Shaft speed of displacement unit in SU2
Note	Throughout the manuscript $\hat{\bullet}$ denotes an estimate of a quantity $\bullet$

References

1. Scheidl, R.; Gradl, C.; Kogler, H.; Foschum, P.; Plöckinger, A. Investigation of a Switch-Off Time Variation Problem of a Fast Switching Valve. In Proceedings of the ASME/BATH 2014 Symposium on Fluid Power and Motion Control, FPMC 2014, Bath, UK, 11–12 September 2014; American Society of Mechanical Engineers Digital Collection: New York, NY, USA, 2014. [CrossRef]
2. Kogler, H.; Scheidl, R.; Schmidt, B.H. Analysis of Wave Propagation Effects in Transmission Lines due to Digital Valve Switching. In Proceedings of the ASME/BATH 2015 Symposium on Fluid Power and Motion Control, FPMC 2015, Chicago, IL, USA, 12–14 October 2015; American Society of Mechanical Engineers Digital Collection: New York, NY, USA, 2016. [CrossRef]
3. Huova, M.; Linjama, M.; Siivonen, L.; Deubel, T.; Försterling, H.; Stamm, E. Novel Fine Positioning Method for Hydraulic Drives Utilizing On/Off-Valves. In Proceedings of the BATH/ASME 2018 Symposium on Fluid Power and Motion Control, FPMC 2018, Bath, UK, 12–14 September 2018; American Society of Mechanical Engineers Digital Collection: New York, NY, USA, 2018. [CrossRef]
4. Midgley, W.J.; Abrahams, D.; Garner, C.P.; Caldwell, N. Modelling and experimental validation of the performance of a digital displacement® hydraulic hybrid truck. *Proc. Inst. Mech. Eng. Part J. Automob. Eng.* **2022**, *236*, 594–605. [CrossRef]
5. Rampen, W.; Dumnov, D.; Taylor, J.; Dodson, H.; Hutcheson, J.; Caldwell, N. A Digital Displacement Hydrostatic Wind-turbine Transmission. *Int. J. Fluid Power* **2021**, *21*, 87–112. [CrossRef]
6. MacPherson, J.; Williamson, C.; Green, M.; Caldwell, N. Energy efficient excavator hydraulic systems with digital displacement® pump-motors and digital flow distribution. In Proceedings of the BATH/ASME 2020 Symposium on Fluid Power and Motion Control, FPMC 2020, Virtual, 9–11 September 2020; American Society of Mechanical Engineers Digital Collection: New York, NY, USA, 2020. [CrossRef]
7. Hutcheson, J.; Abrahams, D.; MacPherson, J.; Caldwell, N.; Rampen, W. Demonstration of efficient energy recovery systems using digital displacement® hydraulics. In Proceedings of the BATH/ASME 2020 Symposium on Fluid Power and Motion Control, FPMC 2020, Virtual, 9–11 September 2020; American Society of Mechanical Engineers Digital Collection: New York, NY, USA, 2020. [CrossRef]
8. Budden, J.J.; Williamson, C. Danfoss Digital Displacement® Excavator: Test results and analysis. In Proceedings of the ASME/BATH 2019 Symposium on Fluid Power and Motion Control, FPMC 2019, Longboat Key, FL, USA, 7–9 October 2019; American Society of Mechanical Engineers Digital Collection: New York, NY, USA, 2020. [CrossRef]
9. Hansen, A.H.; Asmussen, M.F.; Bech, M.M. Hardware-in-the-loop Validation of Model Predictive Control of a Discrete Fluid Power Take-Off System for Wave Energy Converters. *Energies* **2019**, *12*, 3668. [CrossRef]
10. Hansen, A.H.; Asmussen, M.F.; Bech, M.M. Model Predictive Control of a Wave Energy Converter with Discrete Fluid Power Take-Off System. *Energies* **2018**, *11*, 635. [CrossRef]
11. Zagar, P.; Kogler, H.; Scheidl, R.; Winkler, B. Hydraulic Switching Control Supplementing Speed Variable Hydraulic Drives. *Actuators* **2020**, *9*, 129. [CrossRef]
12. Johansen, P.; Hansen, A.H. A Digital Hydraulic Full-Bridge Oscillation Transformer. In Proceedings of the ASME/Bath 2023 Symposium on Fluid Power and Motion Control, Sarasota, FL, USA, 16–18 October 2023; American Society of Mechanical Engineers Digital Collection: New York, NY, USA, 2023. [CrossRef]
13. Michel, S.; Weber, J. Energy-efficient electrohydraulic compact drives for low power applications. In Proceedings of the BATH 2012 Symposium on Fluid Power and Motion Control, FPMC 2012, Bath, UK, 12–14 September 2012.
14. Wiens, T.; Deibert, B. A low-cost miniature electrohydrostatic actuator system. *Actuators* **2020**, *9*, 130. [CrossRef]
15. Stawinski, L.; Skowronska, J.; Kosucki, A. Energy Efficiency and Limitations of the Methods of Controlling the Hydraulic Cylinder Piston Rod under Various Load Conditions. *Energies* **2021**, *14*, 7973. [CrossRef]
16. Zhang, S.; Li, S.; Minav, T. Control and Performance Analysis of Variable Speed Pump-Controlled Asymmetric Cylinder Systems under Four-Quadrant Operation. *Actuators* **2020**, *9*, 123. [CrossRef]
17. Casoli, P.; Scolari, F.; Minav, T.; Rundo, M. Comparative energy analysis of a load sensing system and a zonal hydraulics for a 9-tonne excavator. *Actuators* **2020**, *9*, 39. [CrossRef]
18. Helduser, S. Hydraulische Antriebssysteme mit drehzahlverstellbarer pumpe. *Ölhydraulik Pneum.* **1997**, *41*, 30.
19. Kärnell, S.; Ericson, L. Control of an Asymmetric Cylinder With Two Individually Controlled Pump/Motors. In Proceedings of the ASME/Bath 2023 Symposium on Fluid Power and Motion Control, Sarasota, FL, USA, 16–18 October 2023; American Society of Mechanical Engineers Digital Collection: New York, NY, USA, 2023. [CrossRef]
20. Qu, S.; Fassbender, D.; Vacca, A.; Busquets, E. A high-efficient solution for electro-hydraulic actuators with energy regeneration capability. *Energy* **2021**, *216*, 119291. [CrossRef]
21. Padovani, D. Leveraging Flow Regeneration in Individual Energy-Efficient Hydraulic Drives. In Proceedings of the BATH/ASME 2020 Symposium on Fluid Power and Motion Control, FPMC 2021, Virtual, 19–21 October 2021; American Society of Mechanical Engineers Digital Collection: New York, NY, USA, 2021. [CrossRef]
22. Qu, S.; Zappaterra, F.; Vacca, A.; Busquets, E. An electrified boom actuation system with energy regeneration capability driven by a novel electro-hydraulic unit. *Energy Convers. Manag.* **2023**, *293*, 117443. [CrossRef]
23. Fassbender, D.; Minav, T.; Brach, C.; Huhtala, K. Improving the Energy Efficiency of Single Actuators with High Energy Consumption: An Electro-Hydraulic Extension of Conventional Multi-Actuator Load-Sensing Systems. In Proceedings of the Scandinavian International Conference on Fluid Power, Linköping, Sweden, 1–2 June 2021; pp. 74–89.

24. Siefert, J.; Li, P.Y. Optimal Control of the Energy-Saving Hybrid Hydraulic-Electric Architecture (HHEA) for Off-Highway Mobile Machines. *IEEE Trans. Control. Syst. Technol.* **2022**, *30*, 2018–2029. [CrossRef]
25. Wills, J.; Li, P.Y. Electric and Hydraulic Propel Torque Modulation for a Compact Track Loader With the Hybrid Hydraulic Electric Architecture (HHEA). In Proceedings of the ASME/Bath 2023 Symposium on Fluid Power and Motion Control, Sarasota, FL, USA, 16–18 October 2023; American Society of Mechanical Engineers Digital Collection: New York, NY, USA, 2023. [CrossRef]
26. Chatterjee, A.; Li, P.Y. Human-in-the-Loop Motion Control of a Two-DOF Hydraulic Backhoe Powered by the Hybrid Hydraulic Electric Architecture (HHEA). In Proceedings of the ASME/Bath 2023 Symposium on Fluid Power and Motion Control, Sarasota, FL, USA, 16–18 October 2023; American Society of Mechanical Engineers Digital Collection: New York, NY, USA, 2023. [CrossRef]
27. Schmidt, L.; Hansen, K.V. Electro-Hydraulic Variable-Speed Drive Networks—Idea, Perspectives, and Energy Saving Potentials. *Energies* **2022**, *15*, 1228. [CrossRef]
28. Schmidt, L.; Ketelsen, S.; Hansen, K.V. Perspectives on Component Downsizing in Electro-Hydraulic Variable-Speed Drive Networks. In Proceedings of the Bath/ASME 2022 Symposium on Fluid Power and Motion Control, FPMC 2022, Bath, UK, 14–16 September 2022; American Society of Mechanical Engineers Digital Collection: New York, NY, USA, 2022. [CrossRef]
29. Schmidt, L.; Ketelsen, S.; Hansen, K.V. State Decoupling and Stability Considerations in Electro-Hydraulic Variable-Speed Drive Networks. In Proceedings of the Bath/ASME 2022 Symposium on Fluid Power and Motion Control, FPMC 2022, Bath, UK, 14–16 September 2022; American Society of Mechanical Engineers Digital Collection: New York, NY, USA, 2022. [CrossRef]
30. van Binsbergen-Galán, M.; Schmidt, L. Determination of Load Collective for Sizing of a Hydraulic Drive Network System Considering Simultaneity Between Actuator Loads. In Proceedings of the ASME/Bath 2023 Symposium on Fluid Power and Motion Control, Sarasota, FL, USA, 16–18 October 2023; American Society of Mechanical Engineers Digital Collection: New York, NY, USA, 2023. [CrossRef]
31. Schmidt, L.; van Binsbergen-Galán, M.; Knöll, R.; Riedmann, M.; Schneider, B.; Heemskerk, E. Energy Efficient Excavator Functions Based on Electro-Hydraulic Variable-Speed Drive Network. In Proceedings of the 14th International Fluid Power Conference (14. IFK), Dresden, Germany, 19–21 March 2024; River Publishers Series in Proceedings 2024. [CrossRef]
32. Innas, B.V. *Performance of Hydrostatic Machines—Extensive Measurement Report*; Technical Report; INNAS: Breda, The Netherlands, 2020.

Disclaimer/Publisher's Note: The statements, opinions and data contained in all publications are solely those of the individual author(s) and contributor(s) and not of MDPI and/or the editor(s). MDPI and/or the editor(s) disclaim responsibility for any injury to people or property resulting from any ideas, methods, instructions or products referred to in the content.